

The luminescence properties of rare-earth ions in natural fluorite

M. Czaja · S. Bodył-Gajowska · R. Lisiecki ·
A. Meijerink · Z. Mazurak

Received: 18 June 2011 / Accepted: 2 June 2012 / Published online: 23 June 2012
© The Author(s) 2012. This article is published with open access at Springerlink.com

Abstract For the first time, the luminescence properties of Pr^{3+} , Nd^{3+} and Tm^{3+} and Yb^{3+} ions in fluorite crystal have been obtained by steady-state measurements. In addition, the luminescence spectra of Ce^{3+} , Sm^{2+} , Sm^{3+} , Dy^{3+} , Er^{3+} and Yb^{3+} were measured. It was pointed out that $\lambda_{\text{exc.}} = 415 \text{ nm}$ is most suitable for measuring the Ho^{3+} emission beside the Er^{3+} . The emission of trivalent holmium and erbium ions was measured independently using time-resolved measurements and tentative assignment of luminescence lines to C_{3v} and C_{4v} symmetry sites was proposed. Besides for natural fluorite crystal, the transitions between Stark energy levels of lanthanide ions were presented.

Keywords Photoluminescence · Fluorite · Rare-earth ions · Stark energy levels

Introduction

Fluorite is one of the best-known fluorescent minerals, and its specific properties led G. Stokes to name this phenomenon “fluorescence”. The luminescence of natural fluorite crystals was measured by various methods, among which the photoluminescence (PL) was most often used and significant. The luminescence of fluorite is connected mainly to the presence of rare-earth ions in it. The electrostatic stability of CaF_2 lattice in presence of RE^{3+} ions demands the additional negative charge, mainly as an F^- ion in interstitial sites. The effective symmetry around rare-earth ions could be O_h (for Pr^{3+} , Nd^{3+} , Sm^{3+} , Eu^{3+} , Gd^{3+} , Tb^{3+} , Dy^{3+} , Er^{3+} and Yb^{3+} ions), C_{3v} (for Gd^{3+} , Tb^{3+} , Dy^{3+} , Ho^{3+} , Er^{3+} and Yb^{3+} ions) or C_{4v} (for Ce^{3+} , Nd^{3+} , Gd^{3+} , Tb^{3+} , Dy^{3+} , Ho^{3+} , Er^{3+} and Yb^{3+} ions), what was confirmed by EPR measurements (Weber and Bierig 1964). There has been a large number of research papers on the luminescence of natural fluorite measured by the steady-state method (Illiev et al. 1988; Aierken et al. 2000, 2003; Bodył 2006; Petit et al. 2007; Czaja et al. 2008; Bodył 2009) or the time-resolved method (Gaft et al. 1998, 2001a, b, 2005, 2008). Moreover, the synthetic CaF_2 , BaF_2 and SrF_2 crystals doped with RE ions were investigated intensively (Wood and Kaiser 1962; Kirilyuk 1973; Fenn et al. 1973; Tallant and Wright 1975; Seelbinder and Wright 1979; Chrysochoos et al. 1982, 1983; Illiev et al. 1988; Caldino et al. 1989; Oskam et al. 2002). The splitting of ground and excited levels of Gd^{3+} , Er^{3+} and Ho^{3+} ions were determined, and luminescence lines were assigned to the C_{4v} and C_{3v} symmetry sites on the basis of EPR and electronic optical measurements (Rector et al. 1966; Tallant and Wright 1975; Seelbinder and Wright 1979; Mujaji et al. 1992). In the case of heavy-doped CaF_2 synthetic crystals and their analogues, other luminescence centers, such as pairs or clusters, have been discussed by

M. Czaja (✉) · S. Bodył-Gajowska
Faculty of Earth Sciences, University of Silesia,
ul. Będzińska 60, 41-200, Sosnowiec, Poland
e-mail: maria.czaja@us.edu.pl

R. Lisiecki
Institute of Low Temperature and Structure Research,
Polish Academy of Sciences, Okólna 2, 50-422 Wrocław, Poland

A. Meijerink
Debye Institute, Ornstein Laboratory, University of Utrecht,
Princetonplein 1, Utrecht, The Netherlands

Z. Mazurak
Center of Polymer and Carbon Materials,
Polish Academy of Sciences, M. Skłodowskiej-Curie 34,
41-819 Zabrze, Poland

researchers, too (Fenn et al. 1973; Seelbinder and Wright 1979).

In this paper, we have demonstrated the possibility of steady-state photoluminescence measurement for the purpose of identification of *4f* ions using the mutual relationship between excitation and emission spectra. For the first time ever, the emission and excitation spectra of Pr^{3+} , Nd^{3+} , Tm^{3+} and Yb^{3+} in natural fluorite crystal were investigated by this method. Moreover, we have proposed the most effective excitation for holmium ion emission. Furthermore, the tentative assignment emission line to the respective transition in C_{3v} and C_{4v} symmetry sites was made from the time-resolved spectra of Er^{3+} and Ho^{3+} ions.

Sample properties and measurement conditions

The fluorite crystals studied in this work were found in a lens-like biotite-hornblende pegmatite in Paszowice (Sudety Mountains, Poland). These crystals were transparent and pale yellow, but rather small (1 mm³). The crystal phase was confirmed by X-ray diffraction (Philips PW 3710). The amount of lanthanides was measured by the ICP-MS method in ACME Laboratory (Canada). The marked europium anomaly (0.004) and the plot of REE (rare-earth element) content normalized to chondrite C1 (Fig. 1) are typical for pegmatite fluorite. The

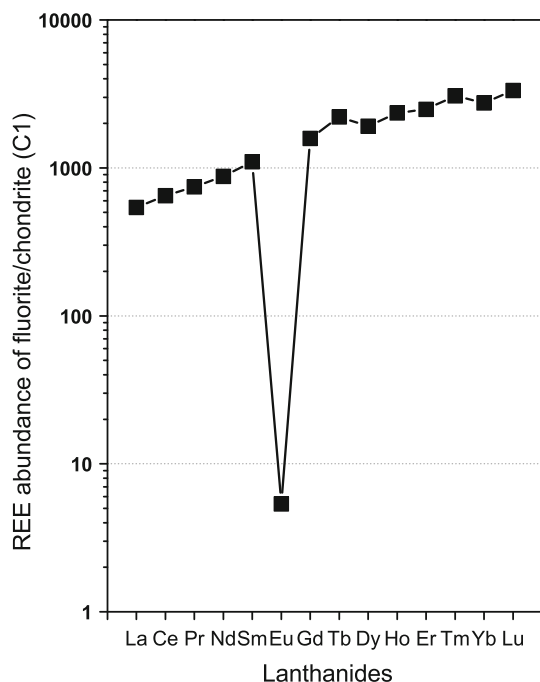


Fig. 1 REE content in fluorite (Paszowice, Poland) normalized to chondrite C1

$\Sigma\text{REE} = 15,765.68$ ppm, $\Sigma\text{HREE} = 14,588.79$ ppm and $\Sigma\text{HREE}/\Sigma\text{LREE} = 12.4$, where *LREE*–light rare-earth element, i.e., La–Eu, *HREE*–hard rare-earth element, i.e., Gd–Lu and Y). However, when the Y is excluded, the contents of light, medium and heavy REE are similar.

To find the most convenient conditions to measure Ho^{3+} luminescence in the presence of Er^{3+} ions, the luminescence spectra of phosphate glass doped by holmium and erbium: 44 % P_2O_5 + 25 % CaO + 15 % BaO + 15 % SrO + 1 % Ho_2O_3 , 44 % P_2O_5 + 25 % CaO + 15 % BaO + 15 % SrO + 1 % Er_2O_3 were synthesized.

Phosphate glasses doped with lanthanide ion or ions can be easily synthesized–easier than CaF_2 crystals. However, the optical properties of *4f* ions in these glasses, especially Ω_i parameters, are different from those in other host materials, although the positions of emission and excitation bands can be treated as a standard (with accuracy measured in \pm nm) in order to identify each particular *4f* ion. We have observed that it is especially useful for Pr^{3+} – Sm^{3+} ions in apatite crystals (Bodył et al. 2009) and for Er^{3+} – Ho^{3+} ions in fluorite and scheelite crystals (Czaja et al. 2008). To enhance the emission of Ho^{3+} ions in the presence of Er^{3+} ions in the spectral range of 550 nm, a 415 nm excitation was chosen. For this excitation, the transition $^5\text{I}_8 \rightarrow ^5\text{G}_5$ of Ho^{3+} ions can be observed besides the transition $^4\text{I}_{15/2} \rightarrow ^2\text{H}_{9/2}$ of Er^{3+} ions. However, the emission from the $^2\text{H}_{9/2}$ level was not measured, in contrast to the emission from $^4\text{S}_{3/2}$.

The steady-state fluorescence measurements for Ce^{3+} , Pr^{3+} , Sm^{3+} , Eu^{2+} , Tb^{3+} , Dy^{3+} , Ho^{3+} , Er^{3+} and Tm^{3+} were performed using a Jobin–Yvon (SPEX) spectrofluorimeter FLUORLOG 3-12 at room and low temperatures using a 450 W xenon lamp, a double-grating monochromator, and a Hamamatsu 928 photomultiplier. Other steady-time measurements were done for Nd^{3+} , Sm^{2+} , Er^{3+} and Yb^{3+} using an Edinburgh Instruments FLS920 spectrofluorimeter with a xenon lamp and Hamamatsu 928 or Hamamatsu R5509-72 photomultipliers or Physik LPD3000 laser (pumped by a Lambda Physik LPX100 excimer laser). The time-resolved emission spectra and decay times were measured using a GDM-1000 double-grating monochromator, equipped with a Hamamatsu 928 photomultiplier. The resulting luminescence signal was stored in a Stanford model SRS 250 Boxcar Integrator coupled with a PC computer. The emission-line accuracy was 0.1 nm. Because the sensitivity of the Hamamatsu 928 or Hamamatsu R5509-72 photomultipliers is almost constant in the range 400–700 nm, no correction curve was needed.

The luminescence decay curves were excited by applying a short impulsive light from an OPO Optical Parametrical Oscillator pumped by the third-harmonic of a YAG:Nd laser. The decay kinetics of excited states were

recorded utilizing a Tektronix model TDS 3052 digital oscilloscope. The decay time and gate width were chosen according to the decay time of each expected luminescence center.

Results and discussion

Steady-state measurements for 4f-5d transitions

The luminescence spectrum of Ce³⁺ ion of the studied fluorite was very similar to those which were known from Aierken et al. (2000) or Bodyl (2009). For λ_{exc.} = 302 nm, the intensive bands at 320 and 343 (336) nm, called by Aierken et al. (2000) A and B, were measured and could be assigned to the transitions from 5d(E_g) → 4f²F_{5/2}) and 4f²F_{7/2}), respectively. The Eu²⁺ ions usually caused a very characteristic blue emission, which was usually measured at 420 nm as the electronic transition 4f⁶5d(E_g) → 4f⁷(⁸S_{7/2}). However, for this crystal, the said emission was not measured, due to a very low Eu concentration (Table 1).

The emission of Sm²⁺ ions was measured at low temperatures (Fig. 2). In fluorite, the excited 4f⁶ level (⁵D₀) is just below the lowest excited 4f⁵5d(E_g) level (Wood and Kaiser 1962), so the energy of the lowest level of te 4f⁵-5d¹ excited electronic configuration could interact significantly with the ⁵D_j levels of the 4f ground configuration and have a strong influence on the optical properties of Sm²⁺. The sharp and intensive emission line at 683 nm (14,641 cm⁻¹) could be attributed to the zero-phonon line (ZPL) of the T_{1u}(4f⁵5d) → A_{1g}(⁷F₀(4f⁶)) transition. Other emission lines at the longer wavelength part of the spectrum, that is, 693 nm (14,430 cm⁻¹), 697 nm (14,347 cm⁻¹) and 699 nm (14,306 cm⁻¹), have a vibronic origin according to the Elcombe and Pryor (1970) and correspond to the ZPL minus the frequency of modes 210, 250 and 355 cm⁻¹, respectively. The emission lines at 708, 720, 730, 748, 761 and 793 nm are assigned to the ⁵D₀ → ⁷F_J (J = 0,1,...,6), and the 365, 452, 467, 485 and 494 nm lines on the excitation spectrum to the 4f⁶(⁷F₀) → 4f⁵(⁶F_J and ⁶H_J)5d(T_{2g}) transitions, respectively.

Steady-state measurements for 4f-4f transitions

Neodymium (Nd³⁺) is one of the most efficient RE centers in minerals, and its characteristic spin-allowed transitions in

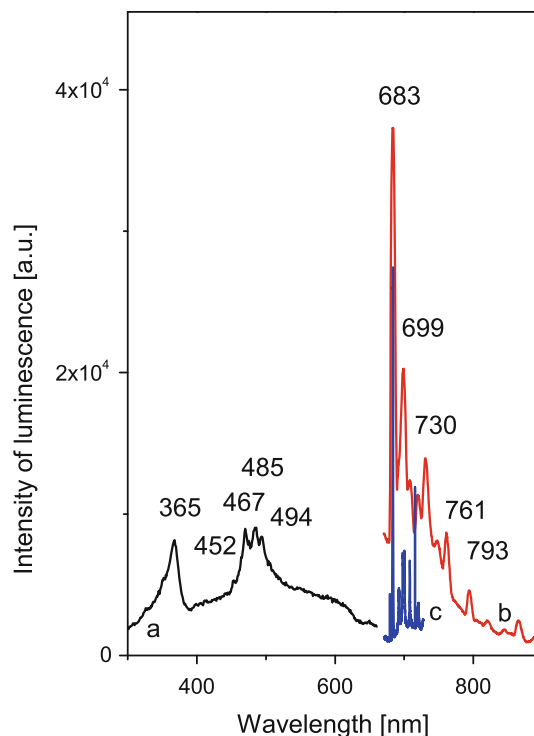


Fig. 2 Luminescence spectra of Sm²⁺: a excitation spectrum monitored at λ_{em} = 682 nm at T = 6 K (black line), b and c emission spectra measured at λ_{exc.} = 485 nm at T = 100 K and T = 6 K, as red and blue lines, respectively

NIR range are ⁴F_{3/2} → ⁴I_{9/2} (864 and 895 nm) and ⁴F_{3/2} → ⁴I_{11/2} (1,065 nm). The NIR emission spectra of Nd³⁺ ion in minerals were measured so far by the time-resolved technique. The steady-state luminescence spectrum of Nd³⁺ ions in our fluorite crystal was measured and presented on Fig. 3. The decay time of the ⁴F_{3/2} state of Nd³⁺ ions in this fluorite had the value of τ = 635 μs. A similarly long decay time of this transition was earlier found in Cs₂NaNdCl₆ [ρ(Nd) = 3.2 × 10²¹ cm⁻³] and in Cs₂NaNd_{0.01}Y_{0.99}Cl₆ crystals (Tofield and Weber 1974) and it amounted to 1.23 and 4.1 ms, respectively. This means that Nd³⁺ ions in our fluorite crystal occupy the O_h symmetry site because only strict octahedral coordination of Nd³⁺ discourages electric-dipole electronic transitions. Subramanian and Mukherjee (1987) predicated that Nd³⁺ ions in fluorite could occupy the O_h and C_{4v} sites.

Moreover, additional emission peaks of Er³⁺ at 1,529 nm (⁴I_{13/2} → ⁴I_{15/2}) and Er³⁺ (⁴I_{11/2} → ⁴I_{15/2}) together with Yb³⁺ (⁴F_{5/2} → ²F_{7/2}) at 978 nm were observed.

Table 1 Abundance (ppm) of rare-earth impurities in natural fluorite from Paszowice, compared with Aierken et al. (2003)

Fluorite	La	Ce	Pr	Nd	Sm	Eu	Gd	Tb	Dy	Ho	Er	Tm	Yb	Lu	Y
Paszowice	142	400	69	401	164	0.3	312	79	468	129	398	76	437	82	12,609
Fluorite Aierken et al. (2003)	270	670	119	678	469	1.1	255	237	1,349	312	927	137	1,010	141	-

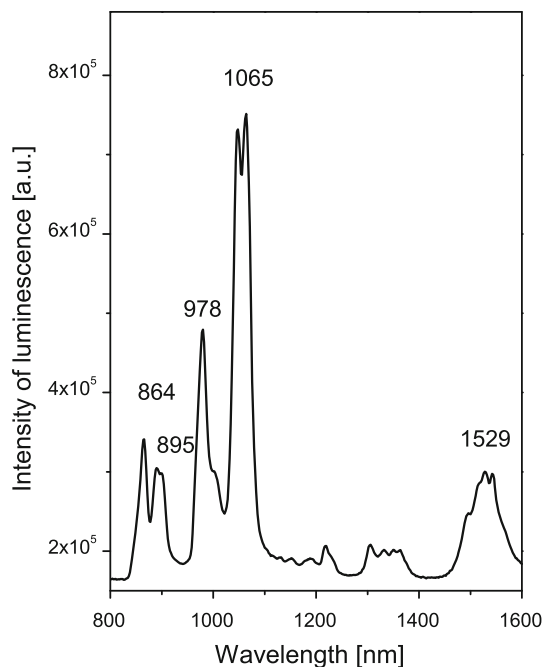


Fig. 3 Luminescence emission spectrum of Nd^{3+} , Yb^{3+} and Er^{3+} measured for $\lambda_{\text{exc.}} = 521$ nm, measured at $T = 300$ K

The luminescence lifetime for $^4\text{F}_{5/2}$ state of Yb^{3+} ion in this fluorite was measured and was equal to $\tau = 9.3$ ms, which was coherent with the results obtained earlier. For the Yb^{3+} ion in C_{4v} site symmetry in synthetic CaF_2 , Petit et al. (2007) have observed that the luminescence lifetime was $\tau = 8$ ms.

For the Pr^{3+} ion, the characteristic emission lines and corresponding transitions are 480–500 nm ($^3\text{P}_0 \rightarrow ^3\text{H}_4$), 650–670 nm ($^3\text{P}_0 \rightarrow ^3\text{F}_2$), 750–770 nm ($^3\text{P}_0 \rightarrow ^3\text{F}_4$), 610–630 nm ($^1\text{D}_2 \rightarrow ^3\text{H}_4$) and ($^3\text{P}_0 \rightarrow ^3\text{H}_6$), 400–410 nm ($^1\text{S}_0 \rightarrow ^1\text{I}_6$). Likewise, some other transitions ($5d-4f$) were measured in the UV region (Gaft et al. 2005). The steady-state luminescence measurements of Pr^{3+} in minerals are difficult because radiative transitions of this ion are hidden by the stronger emission of Sm^{3+} ion (600–650 nm), Dy^{3+} ion (470–490 nm) or Nd^{3+} in the IR range (870–900 nm) (Gaft et al. 2005). It has been noticed (Bodył et al. 2009) that the emission of the Pr^{3+} ion is most intensive for $\lambda_{\text{exc.}} = 442$ nm. For such a condition (Fig. 4), the diagnostic emission lines connected to the $^3\text{P}_0 \rightarrow ^3\text{H}_6$ and $^3\text{P}_0 \rightarrow ^3\text{F}_2$ transitions, appeared at 614 and 641 nm, respectively. Other emission lines on this spectrum (598 and 607 nm) could be assigned to the $^4\text{G}_{5/2} \rightarrow ^6\text{H}_{7/2}$ transition of the Sm^{3+} ion. Chrysochoos et al. (1982, 1983) revealed that Pr^{3+} ions occupied mainly O_h and C_{4v} positions.

The most efficient Sm^{3+} luminescence is usually measured for $\lambda_{\text{exc.}} = 399$ –401 nm (Bodył et al. 2009). The luminescence spectra of our fluorite crystal (Fig. 5) have

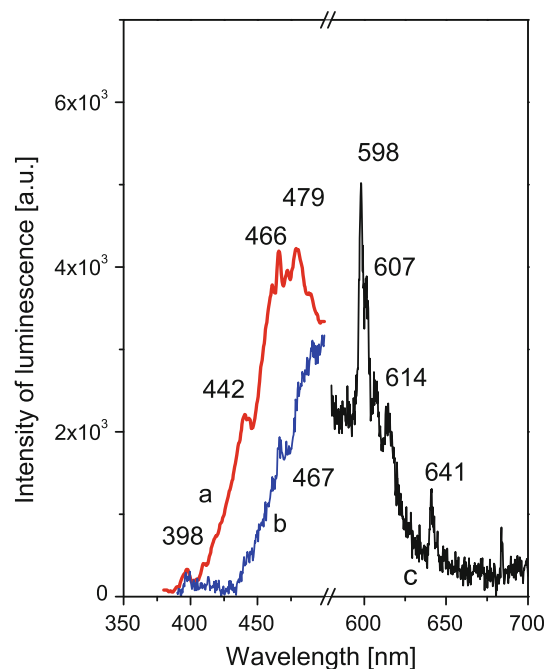


Fig. 4 Luminescence spectra of Pr^{3+} : *a* and *b* excitation spectra monitored at 614 and 641 nm, as red and blue lines, respectively, *c* emission spectrum measured for $\lambda_{\text{exc.}} = 442$ nm, measured at $T = 300$ K (black line)

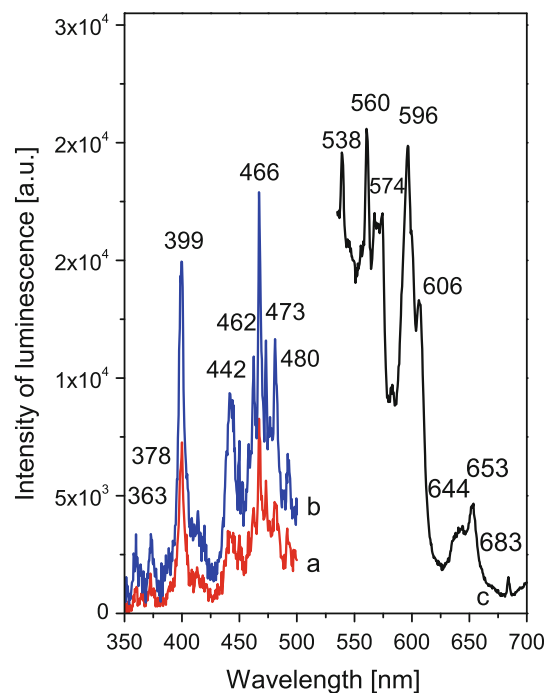


Fig. 5 Luminescence spectra of Sm^{3+} : *a* and *b* excitation spectra monitored at $\lambda_{\text{em.}} = 596$ and 606 nm, as red and blue lines, respectively, *c* emission spectrum measured for $\lambda_{\text{exc.}} = 399$ nm, measured at $T = 300$ K (black line)

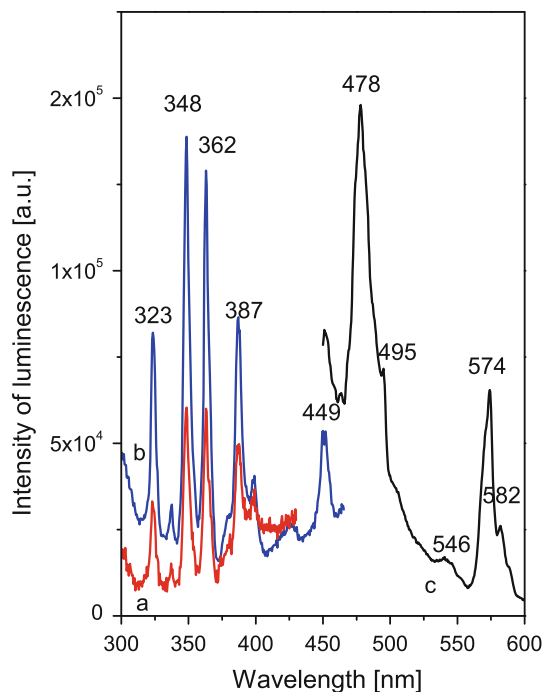


Fig. 6 Luminescence spectra of Dy^{3+} : *a* and *b* excitation spectra monitored at $\lambda_{\text{em.}} = 574$ and 478 nm, as *red* and *blue* lines, respectively, *c* emission spectrum for $\lambda_{\text{exc.}} = 348$ nm, measured at $T = 300$ K (*black* line)

seemed similar to those presented by Aierken et al. (2003). Besides the emission of Sm^{3+} : 560 nm (${}^4\text{G}_{5/2} \rightarrow {}^6\text{H}_{5/2}$), 599 and 606 nm (${}^4\text{G}_{5/2} \rightarrow {}^6\text{H}_{7/2}$) and 644 and 653 nm (${}^4\text{G}_{5/2} \rightarrow {}^6\text{H}_{9/2}$), emission lines of Dy^{3+} at 574 nm (${}^4\text{F}_{9/2} \rightarrow {}^6\text{H}_{13/2}$), Er^{3+} at 538 nm (${}^4\text{S}_{3/2} \rightarrow {}^4\text{I}_{15/2}$) and at 653 nm (${}^4\text{F}_{9/2} \rightarrow {}^4\text{I}_{15/2}$), and Sm^{2+} at 683 nm ($4f^65d \rightarrow 4f^6$) were observed as well.

It was established that the proper $\lambda_{\text{exc.}}$ for Dy^{3+} ion is equal 348 nm. The emission lines at 478 nm (${}^4\text{F}_{9/2} \rightarrow {}^6\text{H}_{15/2}$) and 574 nm (${}^4\text{F}_{9/2} \rightarrow {}^6\text{H}_{13/2}$) were measured (Fig. 6). When other excitation was used, the emission of another ion (or ions) was measured. For example, the emission of erbium ion (542 nm) besides dysprosium ion was measured for $\lambda_{\text{exc.}} = 323, 362$ or 387 nm, while an emission of Sm^{3+} and Pr^{3+} ions was observed for $\lambda_{\text{exc.}} = 449$ nm. On the other hand, for $\lambda_{\text{exc.}} = 348$ nm, Aierken et al. (2003) have shown the emissions of Tb^{3+} as peaks at $495, 546, 582$ and 623 nm. The first three of them were present on our fluorite spectrum (Fig. 6); however, no characteristic excitation lines of the Tm^{3+} ion ($302, 317, 340, 350, 369, 376, 483$ nm) were found on excitation spectra. Instead, for $\lambda_{\text{em.}} = 495$ and 582 nm, the Dy^{3+} lines ($323, 348, 362, 387$ nm) appeared, and for $\lambda_{\text{em.}} = 546$ nm, the excitation lines characteristic for the Er^{3+} ion were observed. It is likely that intensive Er^{3+} emission and excitation lines hide the terbium

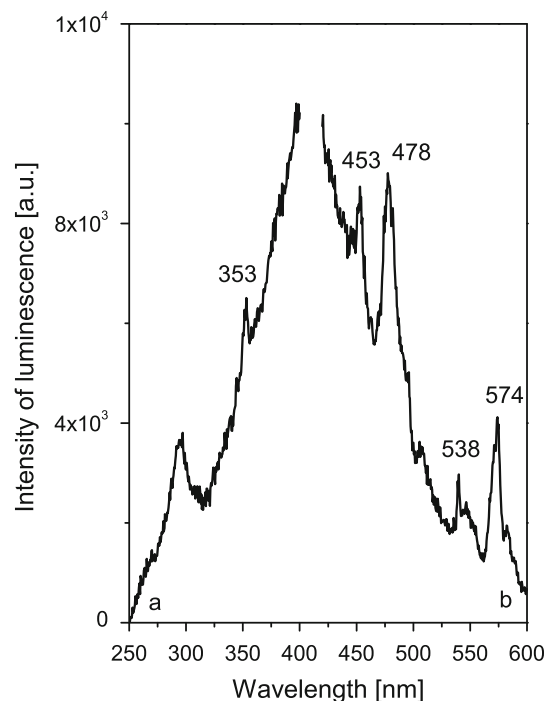


Fig. 7 Luminescence spectra of Tm^{3+} : *a* excitation spectrum monitored at $\lambda_{\text{em.}} = 453$ nm, *b* emission spectrum measured at $\lambda_{\text{exc.}} = 353$ nm, measured at $T = 300$ K

luminescence. Moreover, the complex nature of the 478 nm emission line of Dy^{3+} ion could be seen for other crystals (Bodył-Gajowska 2010).

The Tm^{3+} luminescence for minerals was measured mainly using the time-resolved method (Gaft et al. 2005) or by the cathodoluminescence (CL) technique. In this study, we demonstrate the evident emission of thulium ion (Fig. 7); when $\lambda_{\text{exc.}} = 353$ nm, the transitions ${}^1\text{D}_2 \rightarrow {}^3\text{H}_4$ of Tm^{3+} at 453 nm as well as ${}^4\text{F}_{9/2} \rightarrow {}^6\text{H}_{15/2}$ (478 nm) and ${}^4\text{F}_{9/2} \rightarrow {}^6\text{H}_{13/2}$ (574 nm) of Dy^{3+} ion and ${}^4\text{S}_{3/2} \rightarrow {}^4\text{I}_{15/2}$ (538 nm) of Er^{3+} ion were observed. The concentration of thulium in our fluorite crystal was rather high, but lower than in the crystal of Aierken et al. (2003), so the obtained spectrum could be deemed a success.

The very intensive luminescence of Er^{3+} ion in the VIS and NIR part of spectrum is well known. Under $\lambda_{\text{exc.}} = 377$ nm, strong several lines appear (Fig. 8) and are connected to following electron transitions: 523 nm to ${}^2\text{H}_{11/2} \rightarrow {}^4\text{I}_{15/2}$ and 538 – 554 nm to the ${}^4\text{S}_{3/2} \rightarrow {}^4\text{I}_{15/2}$. The NIR emission spectrum of Er^{3+} was measured at $\lambda_{\text{exc.}} = 521$ nm as 978 (974) nm and $1,529$ nm lines, that is, ${}^4\text{I}_{11/2} \rightarrow {}^4\text{I}_{15/2}$ and ${}^4\text{I}_{13/2} \rightarrow {}^4\text{I}_{15/2}$ transitions, respectively (Fig. 3). The luminescence lifetime for the excited state of the ${}^4\text{S}_{3/2}$ of Er^{3+} ion in this fluorite was measured ($\tau = 436$ μs) and was close to that predicted by the Judd–Ofelt analysis for ${}^4\text{S}_{3/2} \rightarrow {}^4\text{I}_{15/2}$ transition of Er^{3+} ion in

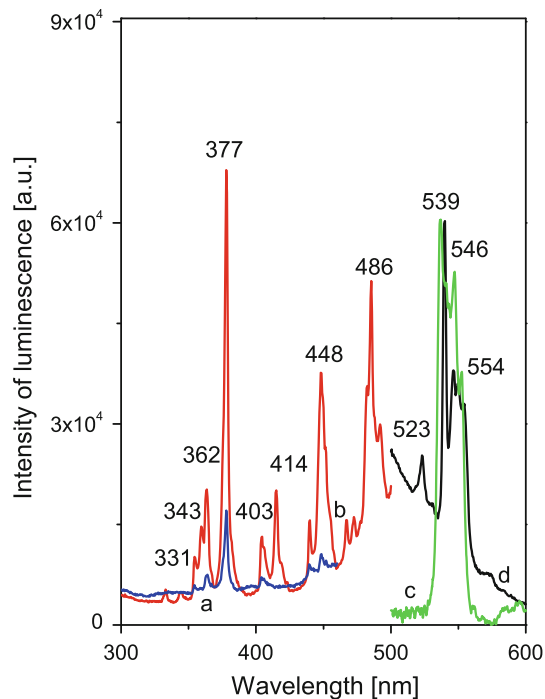


Fig. 8 Luminescence spectra of Er^{3+} : *a* and *b* excitation spectra monitored at $\lambda_{\text{em.}} = 539$ and 523 nm (red and blue lines, respectively), *c* and *d* emission spectra measured for $\lambda_{\text{exc.}} = 415$ nm and for $\lambda_{\text{exc.}} = 377$ nm, (green and black lines, respectively), all measured at $T = 300$ K

phosphate glass (Mazurak et al. 2010). When $\lambda_{\text{exc.}} = 415$ nm is used, emission line 523 nm of the erbium ion disappears almost completely, and the most intensive lines become 536 nm and 552 nm. With excitation at 415 nm ($24,096 \text{ cm}^{-1}$), the ${}^2\text{H}_{11/2}$ at 523 nm ($19,120 \text{ cm}^{-1}$) is some $5,000 \text{ cm}^{-1}$ lower in energy and this gap is too large for a phonon-assisted decay. However, the Er^{3+} levels nearest to 415 nm are ${}^4\text{F}_{3/2}$ and ${}^4\text{F}_{5/2}$ at $\sim 22,300 \text{ cm}^{-1}$ (448 nm), and these can be easily populated as there are few phonons below the pump. It is possible to populate the ${}^4\text{S}_{3/2}$ level via energy exchange mechanisms even for weakly coupled Er^{3+} ions. As a result, an efficient emission is observed from ${}^4\text{S}_{3/2}$, not ${}^2\text{H}_{11/2}$.

The comparison of the emission spectrum of fluorite with spectra of phosphate glasses doped with Er^{3+} and Ho^{3+} (Fig. 9) allows us to conclude that $\lambda_{\text{exc.}} = 415$ nm evidently enhances the green luminescence of Ho^{3+} ions, that is, the ${}^5\text{S}_2 \rightarrow {}^5\text{I}_8$ transition. Aierken et al. (2003) have indicated that the emission line at 553 nm is also characteristic for the ${}^5\text{S}_2 \rightarrow {}^5\text{I}_8$ transition in the Ho^{3+} ion.

The comparison of results for steady-state measurements was put together in Table 2.

Time-resolved measurements

In order to properly identify the origin of emission lines in the 539 – 554 nm part of the spectrum, to assign them to

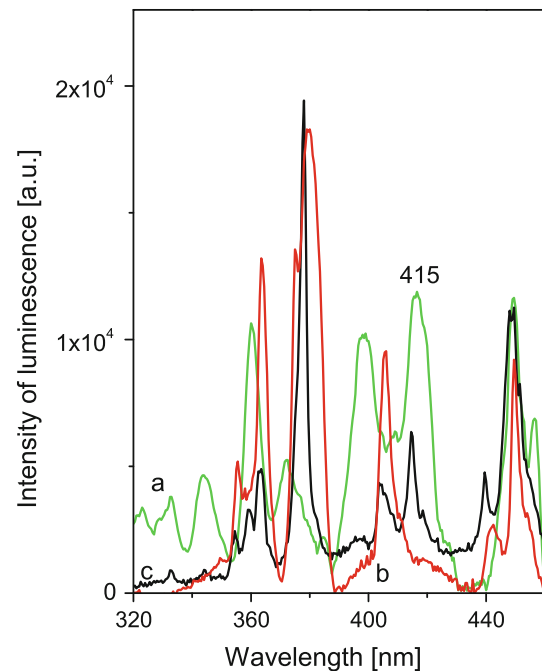


Fig. 9 Excitation spectra of *a* Ho^{3+} doped phosphate glass (green line) and *b* Er^{3+} doped phosphate glass (red line) monitored $\lambda_{\text{em.}} = 552$ nm, *c* of fluorite Paszowice monitored $\lambda_{\text{em.}} = 550$ nm (black line), measured at $T = 300$ K

Er^{3+} or Ho^{3+} ions, and also to determine the crystal sites occupied by these ions in fluorite lattice, time-resolved measurements were performed. The lifetimes for Ho^{3+} 540 nm and Er^{3+} 545 nm emissions measured by Gaft et al. (2001a, b) are similar and equal $5 \mu\text{s}$ and $23 \mu\text{s}$, respectively. When the delay time is $10 \mu\text{s}$ and the gate width $10 \mu\text{s}$, the emission of Ho^{3+} will be observed as well, while the Er^{3+} center is still in the excited state during the time of measurement and does not participate in the emission. By contrast, for delay time $10 \mu\text{s}$ and gate width $30 \mu\text{s}$, the emission of Ho^{3+} will be already quenched, while the emission of Er^{3+} will remain.

On the time-resolved emission spectra, it is normal for the most intensive Stark multiplets to appear. The crystal field can split the energy levels of the RE ion and remove their degeneracy, as the complex character of absorption and emission spectra have often revealed. The number of multiplets, commonly referred to as Stark levels, depends on the quantum number J of ${}^{2S+1}\text{L}_J$ terms and on the crystal site symmetry of the ion. The emission lines belong to transitions between Stark's multiplets of excited and ground levels. The ground level is usually named Z, and the excited levels are designated as “Y, A, B, D, E”, etc. According to these designations, the ${}^5\text{F}_4, {}^5\text{S}_2$ levels of Ho^{3+} and ${}^5\text{S}_{3/2}$ level of Er^{3+} are designated as E. The degeneracy of the ground level of Ho^{3+} (${}^5\text{I}_8$) and of excited ${}^5\text{F}_4, {}^5\text{S}_2$ levels for the tetragonal symmetry site C_{4v} amount to 13

Table 2 The most convenient conditions for steady-state measurements of some RE ions; excitation and emission lines and electronic transitions

λ_{exc} [nm]	Ion: emission line (s) [nm]: transition (s)	λ_{em} [nm]	Excitation line (s)
302	336: Ce ³⁺ : 5d(E _g) → 4f(2F _{7/2})	336	302: Ce ³⁺
485	Sm ²⁺ : 683, 699, 730, 761, 793: 5D ₀ → 7F _J (J = 0, 1, 2, 3, 4)	682	365, 452, 467, 485, 494
521	Nd ³⁺ : 864: 4F _{3/2} → 4I _{9/2} , 1065: 4F _{3/2} → 4I _{11/2} Yb ³⁺ : 978: 4F _{5/2} → 2F _{7/2} , Er ³⁺ : 1529: 4I _{13/2} → 4I _{15/2}	–	Not measured
442	Sm ³⁺ : 598, 607, 614: 4G _{5/2} → 6H _{7/2} , Pr ³⁺ : 641: 3P ₀ → 3F ₂	614 641	442, 466, 479, 490, 442, 466, 479, 490, 398
399	Sm ³⁺ : 560 4G _{5/2} → 6H _{5/2} , 596, 606: 4G _{5/2} → 6H _{7/2} , 644, 653: 4G _{5/2} → 6H _{9/2} ; Er ³⁺ : 538: 4S _{3/2} → 4I _{15/2} , 653: 4F _{9/2} → 4I _{15/2} Dy ³⁺ : 574: 4F _{9/2} → 6H _{13/2}	606 653	363, 378, 399, 442, 451, 466, 473, 480, 363, 377 399, 440, 449, 461, 467, 473, 486
348	Dy ³⁺ : 478: 4F _{9/2} → 6H _{15/2} 574: 4F _{9/2} → 6H _{13/2}	478 574	323, 348, 362, 387, 449
353	Tm ³⁺ : 453: 1D ₂ → 3H ₄ , Dy ³⁺ : 478: 4F _{9/2} → 6H _{15/2} , 574: 4F _{9/2} → 6H _{13/2} Er ³⁺ : 538: 4S _{3/2} → 4I _{15/2}	453	352
377	Er ³⁺ : 523: 2H _{11/2} → 4I _{15/2} 539, 546, 549, 554: 4S _{3/2} → 4I _{15/2}	523, 539 546, 549 554	331, 343, 362, 377, 403, 414, 448, 486
485 (laser)	Er ³⁺ : 520: 2H _{11/2} → 4I _{15/2} 535, 542, 547, 550: 4S _{3/2} → 4I _{15/2} , 666: 4F _{9/2} → 4I _{15/2} Sm ³⁺ : 594, 604: 4G _{5/2} → 6H _{7/2} , 650: 4G _{5/2} → 6H _{9/2}	–	Not measured
270 (laser)	Nd ³⁺ : 850: 4F _{3/2} → 4I _{9/2} , 1047, 1065: 4F _{3/2} → 4I _{11/2} , Yb ³⁺ : 978: 4F _{5/2} → 2F _{7/2} , Er ³⁺ : 974: 4I _{11/2} → 4I _{15/2} , 1529: 4I _{13/2} → 4I _{15/2}	–	Not measured

and 11, while for the trigonal symmetry site C_{3v}-11 and 9. The degeneracy of the excited level for the Er³⁺ ion is double and of ground level it is eightfold, for both symmetry sites.

For low-temperature measurements, the separation of holmium from erbium emission lines was perfectly visible. These lines are shown on Fig. 10a, b for holmium (⁵F₄, ⁵S₂ → ⁵I₈) and erbium ⁴S_{3/2} → ⁴I_{15/2} transitions, respectively. All of these transitions are numbered, counted in [cm⁻¹] and shown in Table 3. The emission lines measured for the fluorite from Paszowice are different from those measured for synthetic crystals by Rector et al. (1966), Dieke (1968), Tallant and Wright (1975), Seelbinder and Wright (1979) or Mujaji et al. (1992). After Seelbinder and Wright (1979) or Mujaji et al. (1992), the most intensive emission lines of the Ho³⁺ ion in the C_{4v} symmetry site were measured at 18,606, 18,490 and 18,448 cm⁻¹ and identified as E₁-Z₁, E₁-Z₄ and E₁-Z₆ transitions, respectively, while for the C_{3v} symmetry site, the most intensive emission lines and transitions were 18,566 cm⁻¹ (E₁-Z₁) cm⁻¹, 18,539 cm⁻¹ (E₁-Z₂),

and 18,501 cm⁻¹ (E₁-Z₃). According to Rector et al. (1966) and Tallant and Wright (1975), the most intensive emission lines of Er³⁺ ion in C_{4v} symmetry site were measured at 18,622, 18,601, 18,539, 18,518 and 18,136 cm⁻¹ and identified as E₂-Z₁, E₂-Z₂, E₁-Z₁, E₁-Z₂ and E₁-Z₆ transitions, respectively, while for the C_{3v} symmetry site, the most intensive emission lines and transitions were at 18,607 cm⁻¹ (E₂-Z₁) cm⁻¹, 18,591 cm⁻¹ (E₁-Z₁), 18,547 cm⁻¹ (E₁-Z₂), 18,364 cm⁻¹ (E₁-Z₃) and 18,319 cm⁻¹ (E₁-Z₅).

There were some difficulties with assigning numerous emission lines to luminescence transitions and comparing them to the values of energy, which are known for synthetic CaF₂:Ho³⁺ or CaF₂:Er³⁺ crystals. Furthermore, some lines are present on the emission spectrum for holmium ion (Fig. 10a) at the shorter wavelength, whose energy should correspond to the transitions from the higher energy sublevels of ⁵F₄, ⁵S₂ excited level (E₁₁₋₉) to the ground ⁵I₈ level (Z₁₋₄), according to Mujaji et al. (1992). Because the population of (E₁₁₋₉) states at T = 10 K is very small, this assumption should be

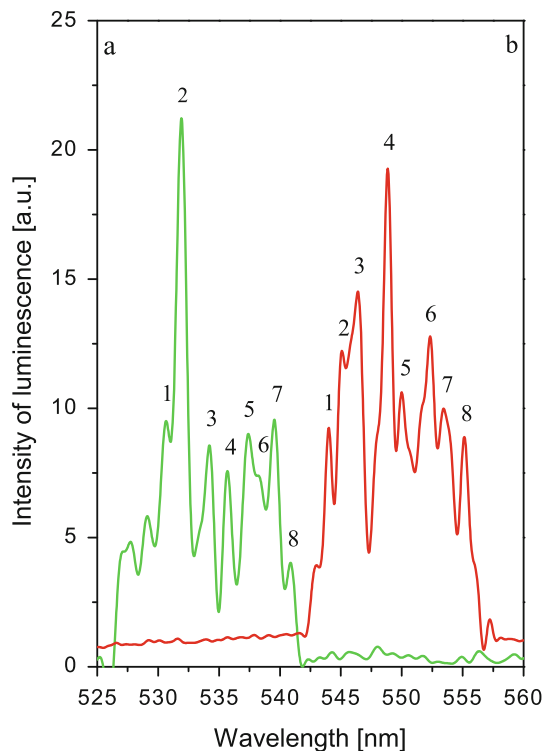


Fig. 10 Time-resolved luminescence spectra of fluorite from Paszowice measured at $\lambda_{\text{exc.}} = 415$ nm; *a* emission lines of Ho^{3+} ; delay time = 10 μs , gate time = 10 μs (green line), *b* emission lines of Er^{3+} ; delay time = 10 μs , gate time = 30 μs (red line), measured at 10 K

rejected. The above discrepancies have led us to accept the assumption that the energies of excited states of Ho^{3+} and Er^{3+} ions in natural crystals are different—insensibly but measurably—from the energies of excited levels in synthetic crystals. The reason for these differences is the different value of local crystal field strength, due to the more complicated chemical composition of a natural fluorite crystal as compared to its synthetic counterpart.

For the Ho^{3+} ion in the fluorite from Paszowice, we have assumed that:

- The excited levels ${}^5\text{F}_4$ and ${}^5\text{S}_2$ are energetically separated, and besides the emission from the ${}^5\text{F}_4$ level, the emission from the ${}^5\text{S}_2$ level was measured as well, as was shown for a few other crystals: YSGG (Pugh et al. 1997), $\text{KGd}(\text{WO}_4)_2$ (Pujol et al. 2001), GdLiF_4 , YLiF_4 and LuLiF_4 (Walsh et al. 2005), YAG (Walsh et al. 2006), YAB (Baraldi et al. 2007) or YGG (Gruber et al. 2009). The ${}^5\text{F}_4$ and ${}^5\text{S}_4$ levels were usually separated in them by an interval of 210–300 cm^{-1} ;
- The splitting of ground ${}^5\text{I}_8$ level (ΔZ) and excited level ${}^5\text{S}_2$ (ΔE) is different in this case than for a synthetic $\text{CaF}_2:\text{Ho}^{3+}$ crystal;

- Similarly to a synthetic $\text{CaF}_2:\text{Ho}^{3+}$ crystal, the most intensive transitions for a holmium ion in a tetragonal site should be $\text{E}_1\text{-Z}_1$ and $\text{E}_1\text{-Z}_4$, but for a trigonal site, they could also be $\text{E}_1\text{-Z}_1$ and $\text{E}_1\text{-Z}_3$.

For the Er^{3+} ion in the fluorite from Paszowice, we have assumed that:

- There are differences in the splitting of the ground ${}^4\text{I}_{15/2}$ level (ΔZ) and the excited level ${}^5\text{S}_{3/2}$ (ΔE) for our fluorite and synthetic $\text{CaF}_2:\text{Er}^{3+}$ crystals;
- the energy of excited level ${}^5\text{S}_{3/2}$ is different (lower) in comparison with a synthetic crystal;
- Similarly to a synthetic $\text{CaF}_2:\text{Er}^{3+}$ crystal, the most intensive transition for erbium ion in a tetragonal site should be $\text{E}_2\text{-Z}_1$, $\text{E}_1\text{-Z}_1$, $\text{E}_1\text{-Z}_2$ and $\text{E}_1\text{-Z}_{5,6}$, but for trigonal site also $\text{E}_1\text{-Z}_1$, $\text{E}_1\text{-Z}_2$ and $\text{E}_1\text{-Z}_3$;
- For the Er^{3+} ion in a CaF_2 crystal, the energy of the Z_4 level could not be identified.

The above assumptions allow us to make a tentative assignment of luminescence lines to a particular transition of holmium and erbium ions in C_{3v} and C_{4v} symmetry sites (Fig. 10; Table 3). The excited level ${}^5\text{S}_{3/2}$ of Er^{3+} has lower energy by about 320 and 240 cm^{-1} for C_{4v} and C_{3v} sites, respectively, whereas the excited level ${}^5\text{S}_2$ of Ho^{3+} has higher energy by about 114 and 37 cm^{-1} for C_{4v} and C_{3v} sites, respectively. The splitting of ground level (${}^4\text{I}_{15/2}$) of the Er^{3+} ion occupying C_{4v} and C_{3v} symmetry sites in synthetic CaF_2 is equal to 84 and 16 cm^{-1} , respectively, while the splitting of the excited level ${}^5\text{S}_{3/2}$ equals 452 and 461 cm^{-1} . For the Ho^{3+} ion in synthetic CaF_2 , it was found that the splitting of the ground level is equal to 512 and 423 cm^{-1} for the C_{4v} and C_{3v} symmetry sites, respectively, while the splitting of the excited level equals 289 and 206 cm^{-1} . From our tentative assignment, the splitting of the excited level for both ions seemed to be generally lower than in a synthetic crystal.

Summary

This study has shown that steady-state measurements can identify the 4f ions in natural crystals. The luminescence of Pr^{3+} , Nd^{3+} and Tm^{3+} ions in fluorite crystal have been received by steady-state measurements; the luminescence of Ce^{3+} , Sm^{2+} , Eu^{2+} , Sm^{3+} , Dy^{3+} , Er^{3+} and Yb^{3+} was measured as well. In comparison with earlier studies on this subject (e.g. Aierken et al. 2003), the intensive luminescence was measured for concentrations of RE ions 1.5–4.0 times smaller. The fluorite crystal studied in this paper is another example of a fluorite for which the violet luminescence did not dominate. Transitions between energy levels of the Ho^{3+} and Er^{3+} ions for a natural fluorite

Table 3 The energy of transitions between Stark's levels—excited and ground—and assignment to C_{4v} and C_{3v} symmetry sites

Emission of Ho ³⁺ ion				Emission of Er ³⁺ ion			
Number of emission line (Fig. 10a)	Emission line at 10 K [cm ⁻¹] (nm)	Site symmetry C _{4v}	Site symmetry C _{3v}	Number of emission line (Fig. 10b)	Emission line at 10 K [cm ⁻¹] (nm)	Site symmetry C _{4v}	Site symmetry C _{3v}
1	18,843 (530.7)	⁵ F ₄ – ⁵ I ₈ or J–Y		1	18,386 (543.9)	–	E ₂ –Z ₁
2	18,804 (531.8)			2	18,347 (545.0)	–	E ₁ –Z ₁
3	18,720 (534.2)	E ₁ –Z ₁	–	3	18,301 (546.4)	E ₂ –Z ₁	E ₂ –Z ₃
4	18,666 (535.7)	E ₁ –Z ₃	–	4	18,220 (548.8)	E ₁ –Z ₁	E ₁ –Z ₃
5	18,603 (537.5)	E ₁ –Z ₄	E ₁ –Z ₁	5	18,181 (550.0)	E ₁ –Z ₂	E ₁ –Z ₅
6	18,574 (538.4)	–	E ₁ –Z ₂	6	18,106 (552.3)	E ₂ –Z ₂	E ₂ –Z ₆
7	18,534 (539.5)	–	E ₁ –Z ₃	7	18,068 (553.5)	E ₁ –Z ₅	E ₁ –Z ₆
8	18,487 (540.9)	–	E ₁ –Z ₆	8	18,013 (555.1)	E ₁ –Z ₆	E ₁ –Z ₇

crystal were measured. The discrepancies between the energy of Stark levels of holmium and erbium ions in synthetic and natural crystals could have been caused by differences in crystal field strength of natural and synthetic crystals. In order to remove any doubt regarding the assignment of the emission transitions and to calculate the energy of Stark levels, it is necessary to measure the energy of transitions from other excited levels of Er³⁺ and Ho³⁺ to ground state and will be the subject of a separate study.

Open Access This article is distributed under the terms of the Creative Commons Attribution License which permits any use, distribution, and reproduction in any medium, provided the original author(s) and the source are credited.

References

- Aierken S, Lee KH, Kusachi I, Yamashita N (2000) Photoluminescence properties of natural fluorite. *J Miner Petrolog Sci* 95:228–235
- Aierken S, Kusachi I, Yamashita N (2003) Natural fluorite emitting yellow fluorescence under UV light. *Phys Chem Miner* 30:478–485
- Baraldi A, Capelleni R, Mazzera M (2007) Hyperfine interaction in YAB:Ho³⁺: a high-resolution spectroscopy investigation. *Phys Rev B* 76:165130–165139
- Bodył S (2006) Luminescencja jonów REE w fluorytach, (in Polish). *Gospodarka Surowcami Mineralnymi* 2(3):347–353
- Bodył S (2009) Luminescence properties of Ce³⁺ and Eu²⁺ in fluorites and apatites. *Mineralogia* 40(1–4):5–18
- Bodył S, Czaja M, Mazurak Z (2009) Optical properties of Pr³⁺, Sm³⁺ and Er³⁺ ions in apatite and phosphate glasses. *Phys Procedia* 2(2):515–525
- Bodył-Gajowska S (2010) Spektroskopia lantanowców w wybranych minerałach. Dissertation, University of Silesia
- Caldino U, de la Cruz C, Munoz H, Rubio O (1989) Ce³⁺ → Eu²⁺ energy transfer in CaF₂. *Solid State Commun* 69:347–351
- Chrysochoos J, Stillman MJ, Jacobs PWM (1982) Laser induced luminescence of Pr³⁺ in CaF₂ attributed to different local site symmetries. In: Silber, Rhyne (eds) *The rare earths in modern science and technology*, vol. 3 McCarthy. Plenum Publishing Corporation, pp 161–164
- Chrysochoos J, Jacobs PWM, Stillman MJ (1983) Laser induced emission spectra of Pr³⁺ in CaF₂ at low temperatures. *J Lumin* 28:177–190
- Czaja M, Bodył S, Głuchowski P, Mazurak Z, Stręk W (2008) Luminescence properties of rare earth ions in fluorite, apatite and scheelite mineral. *J Alloys Compd* 451:290–292
- Dieke J (1968) *Spectra and energy levels of rare-earth ions in crystals*. Wiley, New York
- Elcombe MM, Pryor AW (1970) Lattice dynamics of calcium fluorite. *J Phys C* 3:492–500
- Fenn JB, Wright JC, Fong FK (1973) Optical study of ion-defect clustering in CaF₂:Er³⁺. *J Chem Phys* 59:5591–5599
- Gaft M, Reisfeld R, Panczer G, Blank Ph, Boulon G (1998) Laser-induced time-resolved luminescence of minerals. *Spectrochim Acta A* 54:2163–2175
- Gaft M, Panczer G, Reisfeld R, Uspensky E (2001a) Laser-induced time-resolved luminescence as a tool for rare-earth element identification in minerals. *Phys Chem Miner* 28:347–363
- Gaft M, Reisfeld R, Panczer G, Ioffe O, Segal I (2001b) Laser-induced time-resolved luminescence as means for discrimination of oxidation state of Eu in minerals. *J Alloys Compd* 323–324: 842–846
- Gaft M, Reisfeld R, Panczer G (2005) *Luminescence spectroscopy of minerals and materials*. Springer, Berlin
- Gaft M, Reisfeld R, Panczer G, Dimova M (2008) Time-resolved laser-induced luminescence of UV-vis emission of Nd³⁺ in fluorite, scheelite and barite. *J Alloys Compd* 451:56–61
- Gruber JB, Burdick GW, Valiev UV, Nash KL, Rakhimov SA, Sardar DK (2009) Energy levels and symmetry assignments for star components of Ho³⁺ (4f¹⁰) in yttrium gallium garnet (Y₃Ga₅O₁₂). *J Appl Phys* 106:113110–113112
- Illiev M, Liarokapis E, Sendova MBl (1988) Laser excited luminescence of rare earth impurities in natural and synthetic CaF₂. *Phys Chem of Miner* 15:597–600
- Kirilyuk LV (1973) The concentration dependence of the intensity of the luminescence line at λ = 551.2 nm in single crystals of CaF₂-Ho³⁺ and CaF₂-Ho³⁺ Eu²⁺. *Z Prikl Spekr* 19(5):843–845
- Mazurak Z, Bodył S, Lisiecki R, Gabryś-Pisarska J, Czaja M (2010) Optical properties of Pr³⁺, Sm³⁺ and Er³⁺ doped P₂O₅-CaO-SrO-BaO phosphate glass. *Opt Mater* 32:547–553
- Mujaji M, Jones GD, Syme RW (1992) Polarization study and crystal-field analysis of the laser-selective excitation spectra of Ho³⁺ ions in CaF₂ and SrF₂ crystals. *Phys Rev B* 46:14398–14410
- Oskam KD, Houtepen AJ, Meijerink A (2002) Site selective 4f5d spectroscopy of CaF₂:Pr³⁺. *J Lumin* 97:107–114

- Petit V, Camy P, Doualan JL, Moncorge R (2007) Refined analysis of the luminescent centers in the $\text{Yb}^{3+}:\text{CaF}_2$ laser crystal. *J Lumin* 122–123:5–7
- Pugh VJ, Richardson FS, Gruber JB, Seltzer MD (1997) Characterization and analysis of the $4f$ -electronic states of trivalent holmium in yttrium scandium gallium garnet. *J Phys Chem Solids* 58:85–101
- Pujol MC, Cascales C, Rico M, Massons J, Diaz F, Porcher P, Zaldo C (2001) Measurements and crystal field analysis of energy levels of Ho^{3+} and Er^{3+} in $\text{KGd}(\text{WO}_4)_2$ single crystal. *J Alloys Compd* 323–324:321–325
- Rector CW, Pandey BC, Moos HW (1966) Electron paramagnetic resonance and optical Zeeman spectra of type II $\text{CaF}_2:\text{Er}^{3+}$. *J Chem Phys* 45(1):171–179
- Seelbinder MB, Wright JC (1979) Site-selective spectroscopy of $\text{CaF}_2:\text{Ho}^{3+}$. *Phys Rev B* 20:4308–4320
- Subramanian U, Mukherjee ML (1987) Thermoluminescence spectra and X-ray luminescence spectra of CaF_2 -Ng single crystals. *J Mat Sci* 22:473–477
- Tallant DR, Wright JC (1975) Selective laser excitation of charge compensated sites in $\text{CaF}_2:\text{Er}^{3+}$. *J Chem Phys* 63:2074–2085
- Tofield BC, Weber HP (1974) Efficient phonon-assisted long-lifetime Nd^{3+} luminescence in $\text{Cs}_2\text{NaNdCl}_6$. *Phys Rev B* 10:4560–4567
- Walsh BM, Grew GW, Barnes NP (2005) Energy levels and intensity of Ho^{3+} ions in GdLiF_4 , YLiF_4 and LuLiF_4 . *J Phys Condens Matter* 17:7643–7665
- Walsh BM, Grew GW, Barnes NP (2006) Energy levels and intensity parameters of Ho^{3+} ions in $\text{Y}_3\text{Al}_5\text{O}_{12}$ and $\text{Lu}_3\text{Al}_5\text{O}_{12}$. *J Phys Chem Solids* 67:1567–1582
- Weber MJ, Bierig RW (1964) Paramagnetic resonance and relaxation of trivalent rare-earth ions in calcium fluoride. I. Resonance spectra of crystal fields. *Phys Rev* 234:A1492–A1503
- Wood DL, Kaiser W (1962) Absorption and Fluorescence of Sm^{2+} in CaF_2 , SrF_2 and BaF_2 . *Phys Rev* 126:2079–2088